J Therm Anal Calorim (2012) 107:365–376
DOI 10.1007/s10973-011-1864-3

Thermal properties of 4,4-oxydiphathalic anhydride chitosan filled chitosan bio-composites

Nurhidayatullaili Muhd Julkapli · Hazizan Md. Akil · Zulkifli Ahmad

Received: 25 November 2010 / Accepted: 10 August 2011 / Published online: 23 August 2011

Abstract The 4,4,-oxydiphthalic anhydride-chitosan (ODAC) filler at composition of 2–12 wt/v% was selected to reinforce the Cs matrix by solution casting method. The thermal properties of the bio-composites were then evaluated by thermogravimetry analysis, differential scanning calorimetry, and dynamic mechanical analysis. The addition of ODAC filler in Cs matrix up to 10 wt/v% had increased the thermal stability of the bio-composites by increasing the thermal degradation (T_d) and glass transition temperature (T_g) of the bio-composites. Good interfacial bonds of electrostatic interactions and inter-hydrogen bonds of the bio-composite components significantly influenced the thermal properties of the bio-composites.

Keywords Chitosan · Thermal properties · Bio-composites · Cross linking

Introduction

Chitosan (Cs) is obtained from the most abundant polymer chitin by the alkaline deacetylation. Cs and its derivatives have been used in medical [1], food [2], and in chemical materials [3]. There has been a considerable research interest to prepare Cs film but the scope of preparing pure Cs film has been largely limited due to the thermal and stability performance of Cs [4–6]. A good thermal property toward the application of Cs in various fields is an important factor in guaranteeing acceptable film performance. To improve such properties, Cs has often been coated or supported by incorporation of a rigid filler to make a composite Cs film. Although few, the research articles devoted to Cs-based composites such as metal-based filler [7, 8], mineral-based filler [9, 10], ceramic-based filler [11, 12], bio-polymer-based filler [13, 14], and synthetic polymer-based filler had resulted [15, 16] in an increment of thermal stability of the composites, but the composite method, however, encountered some problems. The main limitation of the Cs-based composites was that the detachment of filler to Cs resulted in incomplete and non uniform coverage of the filler support toward the Cs film.

Therefore, one of the promising approaches to be homogenized with the increase in the thermal properties of the Cs polymer is by single polymer composite technique [17]. This technique is the combination of a matrix and filler derived from same polymer type. Furthermore, because the extent of adhesion between matrix and filler is largely influenced by their physical and chemical compatibilities, this approach is believed to be useful in the enhancement of matrix filler interfacial bonding [17–19].

Meanwhile, cross linking is another approach that has been proven to significantly increase the thermal performance of Cs film [20]. The addition of cross linked segment in Cs film has been used to restrict the flow ability of the Cs polymer chains as heat energy is introduced. Cross-linking approach is used to introduce the rigidity to the Cs polymer where it provides anchoring points for the Cs chains; therefore, these links restrain excessive movement of the polymer chain in the Cs networks. Several cross-linking agents such as glutaraldehyde [21], genipin [22], anhydride acid [23], glutaric aldehyde [24], vanillin [25], and others are currently used to improve various properties of Cs film.

N. M. Julkapli · H. Md. Akil (✉) · Z. Ahmad
School of Material and Mineral Resources Engineering, Universiti Sains, 14300 Nibong Tebal, Pulau Pinang, Malaysia
e-mail: hazizan@eng.usm.my

The aim of this study was to evaluate the potential of the cross linked Cs particle as the reinforcement agent of the Cs-based bio-composites, to optimize the thermal properties of the Cs film. To the best of our knowledge, the combination of both approaches (single composite polymer with the cross linked filler) has not been applied yet. To do so, the dual functional of 4,4′-oxy diphthalic anhydride (ODA) was used as the cross-linking agent to cross link the Cs structure and consequently produced the cross linked 4,4′-oxy diphthalic anhydride-chitosan (ODAC) filler (Fig. 1). The ODAC filler was then applied to reinforce the Cs matrix. The reinforcement effect of ODAC toward Cs matrix was analyzed under their thermal properties by thermogravimetry (TG) analysis, differential scanning calorimetric (DSC), and dynamic mechanical analysis (DMA). Thermal analysis provided information on thermal stabilities and thermal transition of the Cs/ODAC bio-composite films and offered an alternative approach to study the structure of the polymer network as well.

Materials

Cs powder was purchased from Hunza Pharmaceutical (M) Sdn Bhd. 4,4′-ODA as cross-linking agent was purchased from Sigma Aldrich Co and used without further purification. *N*-methyl pyrrolidone (NMP) and acetic acid solvents (AcOH) were brought from Merck (Germany) and distilled at 250 °C and 60 °C before use, respectively.

Methodology

Purification of Cs powder

The commercial Cs (10 g) was dissolved in 1 M AcOH (3 L) by stirring for 12 h. The resulted solution was filtered through 5.0 μm mixed cellulose ester membrane filter to eliminate insoluble matter and Cs was precipitated upon the addition of a concentrated NaOH aqueous solution. Following the extensive washing with water and dried at

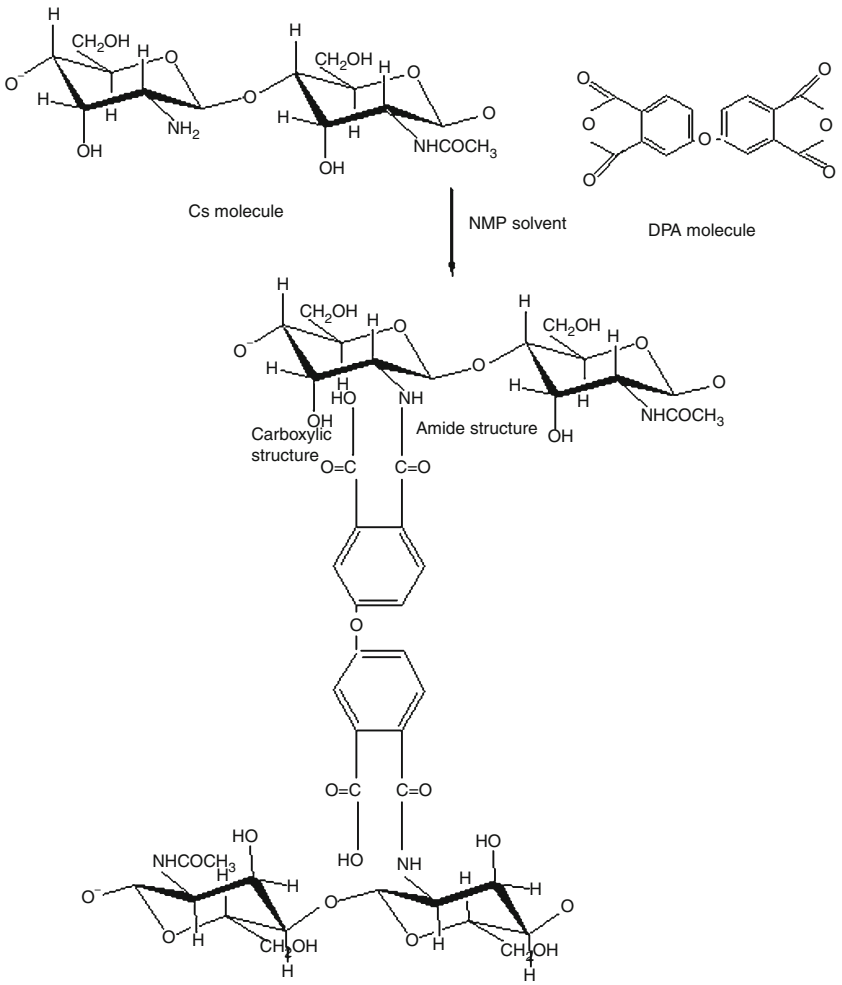

Fig. 1 The chemical structure of ODAC filler

35 °C for 24 h. The purified Cs was milled in a domestic grinder and the fraction of particles having an average diameter lower than 50 μm.

Synthesis of ODAC filler

The preparation method of ODAC filler is almost similar to other cross linked filler [23, 26]. In short, Cs powder (2 g) was first dissolved in AcOH (0.1 M; 100 mL) before being dropped wisely into the solution of NMP and ODA under N_2 flow at 150 °C for 6 h of continuous magnetic stirring (30–50 rpm). The resulting gel was then poured onto a flat glass plate and allowed to evaporate slowly and thermally cross linked at 100 °C for 8 h. The cross linked powder was then manually ground using agate mortar and sieved to a constant size of 20–30 μm before being continuously extracted with the AcOH (0.1 M), methanol, and chloroform.

Preparation of Cs/ODAC bio-composites

The synthesized ODAC powder (at varying portions of 2, 4, 6, 8, 10, and 12 wt/v%) was mixed in AcOH (0.1 M; 100 mL) for 3 h. The pure Cs powder (2 g) was then mixed into the mixture of ODAC and AcOH solution. The mixing process was continued for another 6 h. This continuous stirring (20–30 rpm) was used to expedite the dissolution of Cs powder and to homogenize the solution of the bio-composite mixture. The bio-composites mixture was then poured and casted on the Teflon dish. Each casted film was left dry at room temperature for 24 h. The dried bio-composite films were neutralized by immersing in the dilute NaOH aqueous solution, extensively washed with distilled water and re-dried at room temperature. For simplicity, the different kinds of the Cs/ODAC bio-composite films were expressed as X-ODAC, in which X means the composition of ODAC in the bio-composite.

Characterization techniques

The formation of chemical interactions between the bio-composite components had been characterized by FTIR (FTIR Model: Perkin Elmer, Spectrum One). The Cs/ODAC bio-composite film was first dried at 37 °C until equilibrium of weight was recorded. The IR analysis was then done with a spectrometer in the range of 400–4000 cm^{-1} for 10 times of scanning, under transmitted mode. Thermal properties of the produced bio-composites films were analyzed by thermogravimetic analysis (TG), DSC, and DMA. TG (TG Model: Perkin Elmer, Phyris 7) patterns were measured at heating rate of 10 °C min^{-1} under the N_2 atmosphere over the scanning range of 35–500 °C. Samples of about 10–20 mg were cut into small pieces of 1 mm^3 were used for TG analysis. Both glass transition temperatures (T_g) and the decomposition temperature (T_d) of the bio-composite samples were analyzed by DSC (DSC Model: Perkin Elmer, Phyris 7). DSC thermographs were recorded at heating rate of 10 °C min^{-1} under N_2 atmosphere and heating scan of 35–120 °C for first heating scan process. The second heating scan was done under the heating rate of 5 °C min^{-1} under N_2 atmosphere at heating scan of − 50–450 °C. It should be noted that, 20 μL of aluminum pans with 2–3 mg of samples before used in DSC analysis. The aluminum pans were sonicated in acetone before used. Dynamic mechanical data were obtained with the DMA instrument (Model: DMA 2980 TA instruments). The analysis was done in accordance to ASTM D 4092. All the samples were tested at the heating rate of 5 °C min^{-1} with frequency of 10 Hz under tension mode.

Results and discussion

Preparation of ODAC filler

It is known that Cs can only be dissolved in few kinds of diluting acidic solutions, but as the anhydride-based molecule ODA is usually soluble in some organic solvents such as chloroform, acetone and the like. Cs is insoluble in water and other common solvents due to its strong intramolecular hydrogen bonding [27]. In this study, since the new method employs solvents to form a cross linked structure of Cs and ODA proper solvents should be first taken into account. NMP solvent was selected for ODA component based on its high solubility in water and easily removal characteristic [28]. It was observed that Cs powder could be quite rapidly swollen in low concentration of AcOH (at a concentration of 0.1 M). A sufficient concentration of acidic medium and an appropriate mixing time was required to ensure that all the free NH_2 groups of Cs structure were totally protonized. The complete protonozation of NH_2 groups would result in higher degree of cross linking. Therefore, Cs powder was first firmly and completely dissolved in AcOH before being wisely dropped into the solution of ODA and NMP solvent. Meanwhile, this approach prevents the reaction solution from becoming gelling which consequently, formed a hydrogel. In addition, it was also observed that the formation of cross linked ODA to Cs could not be achieved if an inappropriate molar ratio of components was selected. Therefore, in this study, 2–1 molar ratio of Cs:ODA was selected whereby one molecule of ODA was able to bind with two molecules of Cs. After the drying and grinding process, the ODAC filler appeared as yellowing and odorless powder structure. The extraction process was done in AcOH and acetone to

remove uncross linked Cs and ODA molecules, respectively. Finally, the produced ODAC was completely dried until constant weight was recorded.

Formation of cross linked structure

The formation of covalently amide structure of Cs polymers to ODA cross-linking agent was prepared in accordance with the chemical scheme, as shown in Fig. 1. The cross-linking reaction between Cs molecule and ODA cross-linking agent involves free $-NH_2$ groups of Cs and the $_{R\text{-}\overset{O}{\overset{\|}{C}}=O}$ groups from ODA as the carboxylic-based monomer, ODA, has been found to have a specific nucleophilic in the sense of attacking the NH_2 groups of Cs polymer. In the acidic medium, almost all the NH_2 groups of Cs were positively charged, and they lost the nucleophilicity. This nucleophilicity of NH_2 groups was detected by the protonization state making the reaction pH dependent [29]. Therefore, the reaction was carried out under neutral to mild alkaline conditions (pH 6–7) with the temperature up to 150 °C.

The cross linking might also occur between ODA and OH groups of Cs, because ODA might react slowly with OH groups in Cs since the OH groups are reactive enough to react with ODA. However, due to the negatively electron charged of COOH of ODA molecules, ODA tended to form the covalently bonds with NH_2 rather than OH.

Preparation of Cs/ODAC bio-composites

In order to produce a well dispersion of ODAC in the acidic mediums, high speed mixing was used. The high speed mixers created an intense, concentrated energy input that can disperse ODAC particles significantly quicker than that of lower speed. After obtaining a good dispersion of ODAC particle, Cs powder was added slowly into the mixture. At this stage, the mixing rate was reduced to lower mixing process to limit the formation of micro air bubbles in the mixture. Importantly, the protonization and solubility of Cs matrix were optimized as acidic the mixing process was done in the acidic mediums with p*K*a $\approx$ 6. Generally, the p*K*a of Cs to be completely dissolved is recorded as 6.3–7 [27]. At pH > pKa, the NH_2 groups of Cs are less protonated and the remaining protonated groups available for interaction would result in overall weaker interactions. Moreover, a lower degree of protonization also resulted in Cs powder to appear as aggregate formation. Meanwhile, as the film preparation took place in the acidic mediums, the electrostatic interactions tended to form as compared to inter-hydrogen bonds. In the acidic medium, the protonization process of the NH_2 groups of Cs occurred and ready to bind with the negatively charged COOH groups of ODAC filler and consequently electrostatic interactions between both of composite components was formed (Fig. 2A). Meanwhile, the inter-hydrogen bonds formed at different hydrogen bridge types of Cs matrix and ODAC filler, including; between OH groups, between H of NH–R groups and OH groups, between H of the OH and COOH groups, and between H on the N of the NH–R and COOH groups (Fig. 2B). The analysis of FTIR spectra of the Cs/

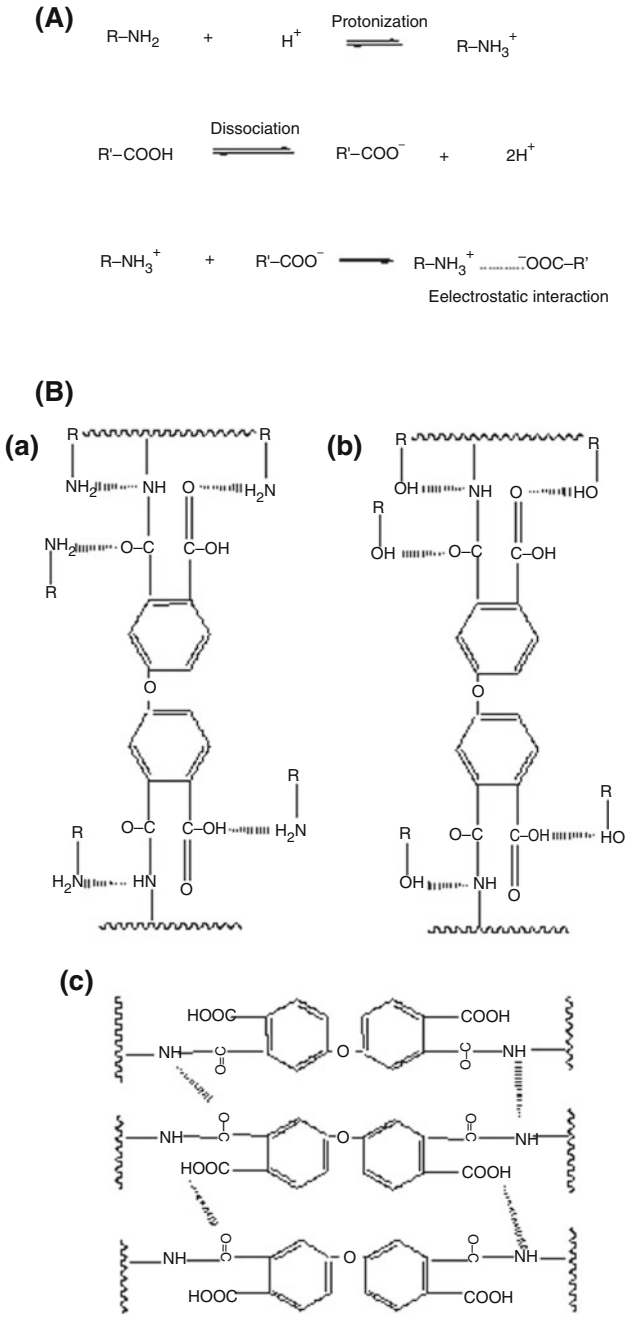

Fig. 2 The formation of interfacial interactions between Cs matrix and ODAC filler *A* electrostatic interactions, *B* inter-hydrogen bonds

ODAC bio-composite film enables these interactions to be identified.

It is noted that the bio-composites mixture of Cs/ODAC could not be formed and casted into film as ODAC filler content was greater than 12 wt/v%. At higher content of ODAC filler, the capability to build agglomeration particle of ODAC is preferred. This may give some hints on the change of the inter-chains in the sample from inter-molecular chains of Cs matrix to ODAC filler to the intra-molecular chains within the ODAC filler. The polar groups of ODAC filler are accessible to interact within the ODAC structures and facilitate the formation of ODAC filler with the larger particle size. This scenario could isolate the dispersion of ODAC filler from Cs matrix, which results in ODAC filler as the domain component in the Cs/ODAC bio-composite system.

FTIR analysis

The chemical composition of Cs/ODAC bio-composition at various compositions of ODAC was analyzed by the FTIR analysis (Fig. 3). The FTIR spectra of pure Cs films showed amide bands at 1659 and at 1559 cm^{-1}, the presence of NH_3^+ at 1628 cm^{-1}, and the saccharine ether peaks of skeletal vibrations involving the C–O stretching between 1130 and 1032 cm^{-1}.

In comparison, the FTIR spectrum of Cs/ODAC bio-composite film was analyzed in Fig. 3. The FTIR spectrum of Cs/ODAC bio-composite film exhibited the characteristic broad amide bands at 1659 and 1559 cm^{-1} and the bending vibrations of oxyl groups at 1387 and 1367 cm^{-1}. Since the ODAC bands overlapped the amide bands of Cs and the imide linkage to ODAC (–C=N–, at 1660 cm^{-1}), the Cs skeletal bands around 1130 and 1032 cm^{-1} were used to detect its presence. Thus, the conclusion can be drawn that the formation of amide as the cross linked structure of ODAC was clearly indicated in all the produced Cs/ODAC bio-composite films.

The NH_2 can be identified by the presence of the two adsorption bands in the NH stretching region arising from the symmetric and asymmetric vibrations of the hydrogen atoms. As shown in Fig. 3, the intensity of the bands at this wave number region increased up to 30% as the composition of ODAC increased in the bio-composite film. On the other hand, hydrogen-bonded alcohol O–H stretching band intensity of the bio-composite film was 43% higher compared to pure Cs film due to the incorporation of ODAC into the polymer structure of Cs. Meanwhile, the C=O stretching region of the amide moiety, between 1600 and 1700 cm^{-1} was quite interesting as it yielded the different signature for pure Cs film and Cs/ODAC bio-composite films. For pure Cs film, the band was split at 1659 and 1628 cm^{-1}. The bands at 1659 cm^{-1} which occurred at similar wavelengths in polyamides and proteins is commonly assigned to starching of the C=O group hydrogen bonded to N–H of the neighboring intra-sheet chain. Regarding the 1621 cm^{-1} bands, which are not present in polyamides and proteins, its occurrence may indicate a specific hydrogen bond of C=O with the hydroxymethyl group of the next Cs monomer of the same polymer chains.

The formation of electrostatic interactions of Cs matrix to ODAC filler was proven by the presence of the band at 1413 cm^{-1} that was attributed to the $–NH_3^+$ groups of the Cs matrix interacting with COO– groups of ODAC filler.

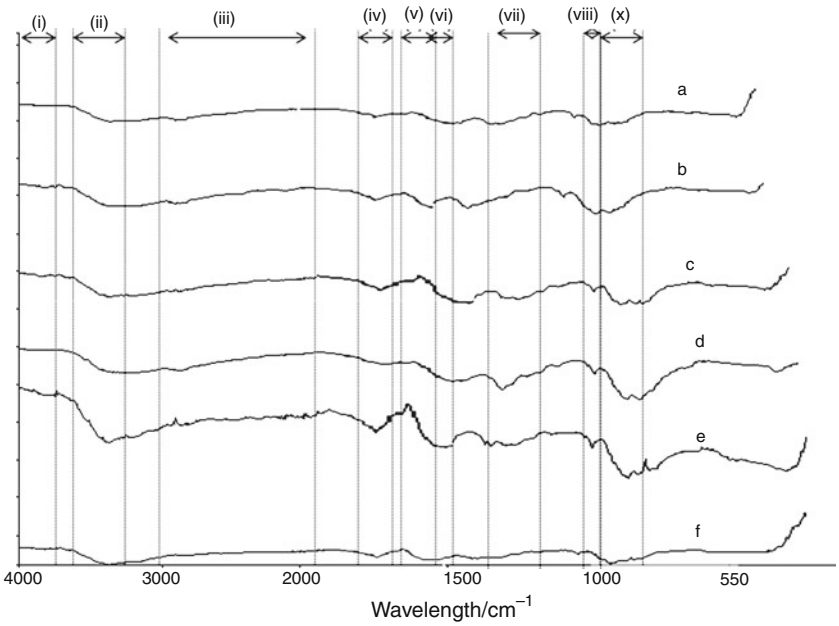

Fig. 3 The FTIR analysis of Cs/ODAC bio-composites with corresponds to different ODAC filler loading *a* 0 ODAC, *b* 2 ODAC, *c* 6 ODAC, *d* 8 ODAC, *e* 10 ODAC, *f* 12 ODAC

Meanwhile, the formation of electrostatic interaction was illustrated by an increment of intensity and blue-shift of the 2500 cm^{-1} (NH_3^+), 1450 cm^{-1} (asymmetric COO^-), and 1408 cm^{-1} (symmetric COO^-) peaks with the addition of 2–8 wt/v% content of the ODAC filler. In fact, the C=O stretching band of ODAC at 1731 cm^{-1} shifted to 1597 cm^{-1} for carboxylate anion as the composition of ODAC filler increased. The peak height of the respective peaks also increased approximately up to 25% as 8 wt/v% of ODAC filler was incorporated into the Cs matrix.

A good interfacial region of the matrix to filler became important as the thermal energy was subjected to shift through the Cs/ODAC bio-composite components.

TG analysis

TG and its derivative curves of Cs/ODAC bio-composites with respect to different composition of ODAC are shown in Fig. 4. While, the temperatures for the occurrence of the main thermal events and corresponding *mass losses* are given in Table 1. The derivatives TG deals with the *mass* change with respect to temperature (d*W*/d*T*) and simultaneously obtained from TG. Generally, the TG analysis curves of the Cs/ODAC bio-composite films show two steps of degradation.

The first thermal event occurred at the temperature range between 25 and 140 °C, where all the produced bio-composite films showed a *mass loss* ranging from 10 to 12%. The rate of *mass loss* increased with the increase in temperature and attained a constant *mass loss* at the temperature ranging from 114 to 240 °C. This is attributed to the evaporation of water, whose content affect the function of the morphology, crystallinity, and hydrophilicity of the Cs polymer. According to the results presented in Fig. 4, the *mass losses* corresponding to the evaporation of water seem to depend on the composition of ODAC filler in the bio-composite films. In this sense, one can observe that derivative with higher content of ODAC presents a lower *mass loss* in this temperature interval. Meanwhile, a little variation in the location of the resultant peaks was observed for different loading of ODAC filler. This variation was attributed to the adsorption ability of the Cs/ODAC bio-composites toward the surrounding moisture. Cs matrix with two types of polar groups (NH_2 and OH) tends to have more hydrophilic character as compared to ODAC filler.

The second thermal event occurs in temperature range of 240–400 °C. As shown in Fig. 4, the data and marked vertical bars present their T_{onset} of this respective degradation temperature. It is interesting to note that with regard to composition of ODAC filler, the bio-composite film containing a greater amount of ODAC filler has the lowest *mass loss.* This case is acceptable with the bio-composite film with lower ODAC composition of 10 wt/v%. The cross-linking structure of ODAC filler widening the decomposition process up to the heating temperature of

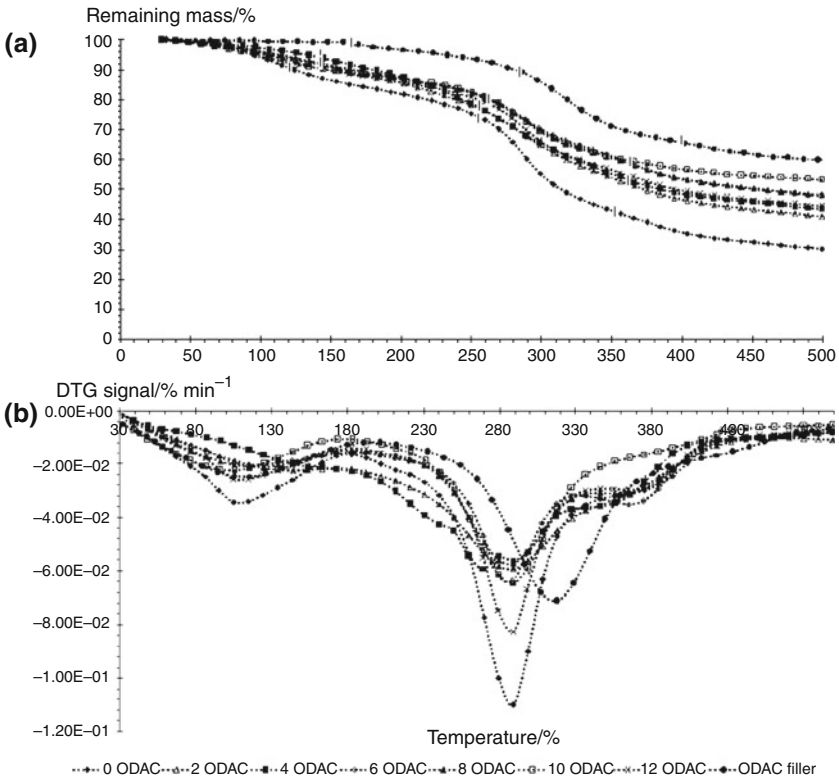

Fig. 4 The TG analysis of Cs/ODAC bio-composites **a** the mass loss over temperature curves, **b** derivative *mass loss* over temperature curves with corresponds to different ODAC filler loading

Table 1 The TG analysis of Cs/ODAC bio-composites regarding the T_{onset}, T_{offset}, and mass loss

Samples	T_{onset}/°C	T_{offset}/°C	Mass loss/%
1st Degradation stage			
0 ODAC	45	119	16
2 ODAC	46	121	16
4 ODAC	45	121	16
6 ODAC	46	122	16
8 ODAC	46	121	15
10 ODAC	45	122	14
12 ODAC	46	123	14
ODAC filler	48	124	17
2nd Degradation stage			
0 ODAC	146	398	32
2 ODAC	148	391	37
4 ODAC	147	391	49
6 ODAC	148	392	47
8 ODAC	149	392	49
10 ODAC	150	389	55
12 ODAC	149	389	56
ODAC filler	148	394	60

300 °C for 10 ODAC while only 220 °C for 0 ODAC sample. Meanwhile, the degradation steps of other samples located within the 0 ODAC and 10 ODAC samples. Therefore, 10 ODAC was recorded as the bio-composite with the highest thermal stability. The degradation temperature had influenced the effect of cross linked filler on the thermal stability of the polymer network structure since Cs matrix is a polymer with linear chains. The 0 ODAC sample prepared from the solvent evaporation process involved a weak network structure due to inter-molecular hydrogen bonding between OH groups as well as NH_2 groups. The insertion of ODAC filler into Cs matrix changed the regularity of the polymer network by inducing not only inter-hydrogen bonds but also electrostatic interaction, and to some extent, increased the thermal stability of the sample. In addition, the NH-R structure formed as the cross linked bridge in ODAC network has good thermal stability, which led to lower decomposition rate of the samples. The effects of NH-R groups were also reflected in the residual *mass* of the bio-composite film in TG. For example, at 350 °C, 58% of *mass losses* were obtained for 0 ODAC sample, whereas 30% of weight losses for 10 ODAC sample. Generally, the degradation mechanism starts with the elimination of OH and NH_2 groups from the cyclic structure in the structural unit of Cs and ODAC. Consequently, the interaction bonds of Cs matrix to ODAC filler were completely destroyed and had caused both bio-composite components to become an individual component. At this stage, acetic acid, butyric acids, and a series of lower fatty acid were formed due to the split of the individual Cs and ODAC glycoside linkage [5, 30]. Consequently, as the heating temperature rose up, the breakage of the main chain of Cs and ODAC consequently occurred.

Finally, it is interesting to note that the TG thermograph of the Cs/ODAC bio-composite films were located between those of ODAC filler and neat Cs film. In general, if two components of the composite have a significant difference in their T_{onset} and no interaction exists between them. The TG thermograph of the bio-composite would show its thermal degradation in two stages matching the T_{onset} of each component [31]. However, as shown in Fig. 4, all the produced bio-composite samples have only one T_{onset}, suggesting that a considerable amount of interactions may exist between the two components in each mixture, which most probably come from the inter-hydrogen bonds and electrostatic interaction of the composite components. In addition, the curves in Fig. 4 register that T_{onset} of the bio-composite measurably changed with the composition proportion but higher than T_{onset} of Cs and lower than T_{onset} of ODAC. These results indicated that these two components were well bound together with a good interfacial bonding. The inter-penetration between these two bio-composite components should enhance the thermal stability of the Cs film.

DSC analysis

The DSC thermograph of Cs/ODAC bio-composites with respect to different ODAC filler loading are viewed in Fig. 5, respectively. These plots represent the dependence of the calorimetric parameters of volume phase transition (transition temperature, enthalpy, heat capacity increment, and width) for the Cs/ODAC bio-composites at various compositions of ODAC filler loading.

Generally, all the bio-composite samples showed broad endothermic peak in the temperature range of 100–120 °C for first heating scanning (Fig. 5). The endothermic peaks corresponded to the loss of water which was associated with the hydrophilic nature of the sample. They involved a single narrow asymmetrical peak of heat capacity in the temperature range of the evaporation process. It is of importance to highlight that in all cases, the apparent partial heat capacity of polymer network in the bio-composite sample was smaller than that in the nature Cs film. This indicated the formation of hydrophobic part of the bio-composite sample pursuant to reduction in the water-holding capacity. The amount of the phase transition of water in the bio-composite sample was calculated by enthalpy of fusion in the temperature ranging from 100–120 °C. It was reported that the water molecules formed a complex structure with the polymer chains of

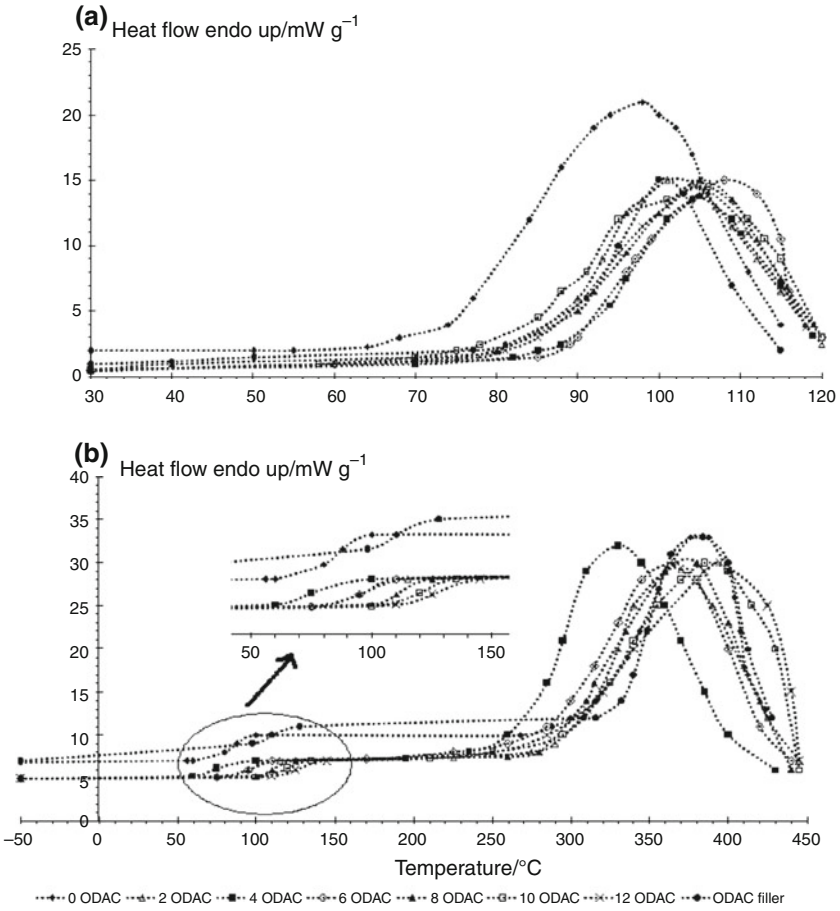

Fig. 5 The DSC analysis of Cs/ODAC bio-composites at **a** first heating scan and **b** second heating scan with corresponds to different ODAC filler loading

hydrophilic polymer through inter-hydrogen bonds [32, 33]. The enthalpy fusion of pure water was recorded as 333 J/g [31]. As shown in the DSC thermographs of first heating scan (Table 2; Fig. 5), the resultant enthalpy fusion of water content for all samples was greater than that of pure water. Therefore, it can be considered that inter-hydrogen bonds between the water molecules and the polar groups of the bio-composites components had taken place, reflecting the adsorption capability of the bio-composite sample.

In the second heating scan, two endotherm peaks were obviously occurred (Fig. 5b)). The endothermic peaks were associated to the glass transition temperature (T_g) and degradation temperature (T_d). For the first heating scan, only single T_g was recorded, located between the T_gs of native Cs (0 ODAC) and ODAC filler. The T_g values indicate as the samples are heated to cause a change from the glassy state to the rubbery state. This is an indication that Cs matrix and ODAC filler create a miscible system and most probably that ODAC filler is homogenously dispersed in molecular level into the Cs matrix. Furthermore, enthalpy relaxation of the bio-composite films was approximately 23% increased with the addition of 8 wt/v% of the ODAC filler, indicating that the molecular mobility of the bio-composite system was increased in the presence of ODAC. Meanwhile, the observed T_g values of the bio-composite did seem to exhibit a significant relationship with the composition of ODAC filler. It clearly indicated that transition temperature of the 2 ODAC and 4 ODAC coincided with that of the 0 ODAC sample (with less than 5% of differences) thus it is reasonable to believe that the intrinsic properties of the bio-composites samples are insignificantly changed due to the addition of ODAC at below than 4 wt/v%. In this case, the cross linked structure of ODAC sustained the Cs matrix in place without any movement of the Cs polymer chain at approximately 10 °C after the T_g of the pure Cs film (0 ODAC). In addition, the similarity in the transition shapes (as correspond to their length and width) of 0, 2, and 4 ODACs should mean the equality of the specific transition enthalpy and heat capacity of the respective samples (Table 2). The constant in transition temperature, transition enthalpy, and heat capacity of the respective samples indicated that only a small part of the bio-composite was affected due to the presence of the cross linked structure of ODAC.

However, as the composition of the ODAC increased up to 6–10 wt/v%, there was a significant increment of about 12% on the transition temperature, transition enthalpies and

Table 2 The DSC of Cs/ODAC bio-composites regarding at first and second heating scans

Samples	T_{onset}/ °C	T_{peak}/ °C	T_{offset}/ °C	ΔH_a H/ J g^{-1}	Energy/ mJ
1st Heating scan/T_w					
0 ODAC	83	104	108	351	702
2 ODAC	81	103	116	350	701
4 ODAC	83	105	119	348	697
6 ODAC	82	106	113	348	696
8 ODAC	81	105	114	346	692
10 ODAC	85	110	112	346	693
12 ODAC	93	110	113	342	684
ODAC filler	92	112	111	341	682
2nd Heating scan/T_g					
0 ODAC	47	51	60		
2 ODAC	48	52	61		
4 ODAC	49	54	63		
6 ODAC	50	56	64		
8 ODAC	52	57	64		
10 ODAC	51	58	66		
12 ODAC	52.	58	68		
ODAC filler	57	63	69		
2nd Heating scan/T_d					
0 ODAC	250	262	315	823	1646
2 ODAC	254	324	379	832	1664
4 ODAC	261	325	382	837	1675
6 ODAC	279	327	379	829	1658
8 ODAC	283	325	378	828	1657
10 ODAC	291	326	380	831	1662
12 ODAC	290	32	381	827	1655
ODAC filler	274	367	389	824	1648

heat capacity of the bio-composites samples. The resultant T_g could be due to the restricted mobility of the Cs molecules in the presence of the cross linked structure of ODAC molecules. The electrostatic and inter-hydrogen bonding between Cs and ODAC molecules was chemically changed conformation of the bio-composite structure, assuring a better resistance of the polymer chains (Fig. 2A, B). Hence, it seemed that effects of this transition temperature were related to trivial elasticity of the bio-composites components which were induced by the introduction of ODAC filler.

Meanwhile, the transition width (as determined by the breadth of the transition heat capacity of the transition) for 12 ODAC was considered 34% broader as compared to other Cs/ODAC bio-composite samples. This may be due to the microphase on the interfacial region of ODAC filler to Cs matrix. At this point, ODAC tended to form inter-hydrogen bonding between them rather than with Cs matrix. The microphase separation gave rise to the formation of ODAC domains. Therefore, most of Cs matrixes that were located in the outer layer of the ODAC domains did not participate in the transition registered by the DSC analysis. Evidently, the resultant transition temperature of 12 ODAC sample was recorded at the nearer point of ODAC powder. This agreement seemed to indicate a similarity of local structure of the ODAC powder and the ODAC domains in the 12 ODAC sample. Hence, the greater the transition width means the greater the transition cooperatively. Therefore, this finite width of the transition in 12 ODAC sample reflects the fact that the system under consideration consisted of the microscopic region between its components which consequently had caused all the composite components of the system to undergo the phase transition almost independently. Thus, broadening of the transition was observed for both ODAC fillers, and 12 ODAC sample was considered to have similar behavior.

The second endothermic peaks of the second heating scan occurred at the temperature range of 250–450 °C and identified as degradation temperature (T_d). The T_d of samples involved pyrolysis, split, and break of the Cs polymer chains. As shown in Fig. 5, no significant different can be observed between the onset temperature of the degradation event. This revealed that the insertion of ODAC filler into Cs matrix did not affect the degradation process of the sample. Cs matrix and ODAC filler are two different systems. As mentioned before, the electrostatic interaction and inter-hydrogen bonds provided the Cs/ODAC bio-composite film with a good interfacial bonding (Fig. 2A, B). The good interfacial bonding make them become a bio-composite system with reduction in the free energy. Therefore, the degradation process takes place between that of Cs matrix and ODAC filler.

Dynamic mechanical analysis

The relationship between heating temperature and the storage modulus for the Cs/ODAC bio-composite film with different composition of ODAC filler is shown in Fig. 6a. Generally, the storage modulus of samples starts with the highest point in the DMA curves. However, the further increase of the heating temperature caused a significant decrease in storage modulus, which was indicative of the polymer motion by mechanical shear. Since, the Cs matrix is an unstable structure that may undergo densification due to the thermal movement of the Cs polymer chains at the higher temperatures [32], the addition of ODAC, therefore, tends to increase the stability of Cs film at an evaluated temperature. As ODAC was incorporated in Cs matrix, more stable structures of Cs matrix were formed, and as a

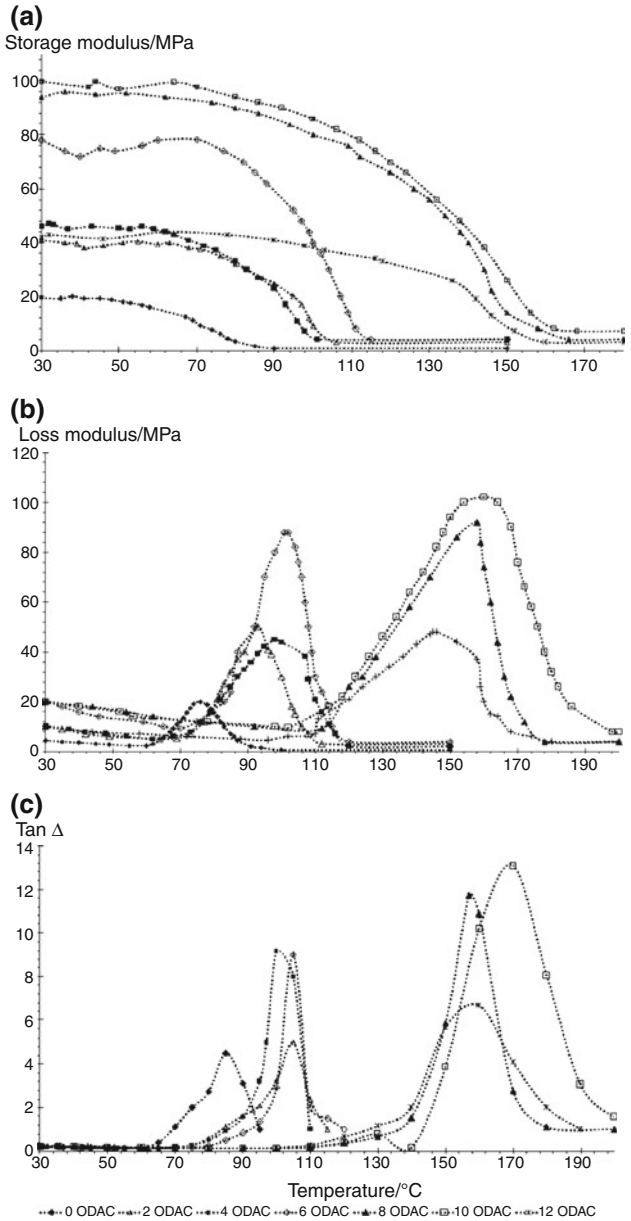

Fig. 6 The DMA analysis of Cs/ODAC bio-composites results with **a** storage modulus, **b** loss modulus, and **c** tan ΔH_a with corresponds to different ODAC filler loading

result, no great reduction in storage modulus of the Cs film was observed. It was observed that the storage modulus peak temperature for Cs/ODAC bio-composite films shifted to a higher temperature as the amount of ODAC fillers was added. The results were associated to the rigidity of the ODAC filler and Cs matrix molecular chains. The storage modulus data suggested that the covalent bond of ODAC cross linked structure changed the microstructure of the Cs matrix and that may affect the Cs polymer to be retained at the higher heating temperature.

The loss modulus of the Cs/ODAC bio-composites films is shown in Fig. 6b. Each of Cs/ODAC bio-composite samples had only one obvious peak, indicating that there was no noticeable phase separation in the bio-composite system. This result collated well with the TG and DSC analysis. Meanwhile, Fig. 6b also indicates a sharper and smaller peak observed for the bio-composite with the less amounts of ODAC. Cs is highly crystalline bio-polymer with the presence of inter-hydrogen bonds. ODAC is an amorphous polymer due to the cross linked structure. Therefore, additions of ODAC filler induced the amorphous behavior in Cs matrix, which were reflected in widen and broaden of the respective peak of the sample. As discussed before, the inter-chain space of Cs might be expanded due to the broken linkage of its inter-hydrogen bonds, which resulted in a reduction of the loss modulus after T_gs value.

Figure 6c indicates the tan ΔH_a behavior of the Cs/ODAC bio-composite with the respect of different loading of ODAC filler. The tan ΔH_a value was derived from the value of loss modulus divided by value of storage modulus at the specific temperature. T_g is identified as the optimum values of the respective tan ΔH_a peaks. From Fig. 6c, the T_gs of the bio-composite increases with increasing of the ODAC content. Initially, the T_g value of the pure Cs film was recorded at 80 °C. This value increased almost 47% with incorporation of 2–10 wt/v% of the ODAC filler. However, addition of 12 wt/v% of ODAC filler reduced almost 12 °C with the ones obtained from the previous composition. The increment of T_gs for the produced bio-composites must results from the ODAC molecules which enter Cs continuous phase; to restrict the movement of the Cs matrix. Lot of studies had demonstrated that molecular mobility was the most important factor affecting the thermal stability of the bio-composite [34–36]. The mobility of the Cs/ODAC polymer chains increased with increasing analyzed temperature, which led to an increase in both free volumes of the polymer networks and the motion rate of the polymer molecules. These led to an increase of the driving force of the phase transformation of the Cs/ODAC bio-composite film. At this point, freer space might be formed to induce the flowing process. ODAC particle reduced the flexibility of the Cs matrix and produced more stable structures of sample, and therefore, the bio-composite film with higher composition of ODAC filler was supposed to show greater values of T_g. Intra- and inter-molecular interactions of the Cs/ODAC bio-composite system may be explained as: at the lower composition of ODAC filler, inter-molecular interaction was performed between Cs matrix and ODAC filler. While, the intra-molecular interaction tends to occur at the higher composition of ODAC filler. The intra-molecular interaction involves either the interaction of ODAC to ODAC filler or Cs to Cs matrix. It is of interest to highlight that Cs/ODAC bio-composite system containing two different segments;

soft segment contributed by Cs matrix while hard segment contributed by ODAC filler. It is evident that the micro-phase separation between the hard and soft segment in the bio-composite system must enhance the movement of the Cs matrix to make great shift of T_g. The improved resultant T_g values could be ascribed to the improved interfaces between the ODAC filler and the cross linked structure of ODAC.

Conclusions

The Cs/ODAC bio-composite is considered as the compatible system of bio-composite due to the:

1. FTIR spectra demonstrated the presence of the electrostatic interactions and hydrogen bonds of the bio-composite components.
2. Addition of ODAC shifted the main decomposition peak position to higher temperature side and therefore, improved the thermal stability of the Cs/ODAC bio-composite films.
3. All the single T_g values for the bio-composite are in excellent agreement with the value of 120–150 °C has been indicated by DSC and DMA.

Acknowledgements Appreciations are given to Fundamental Research Grant Scheme (FRGS 6070024) under Ministry of Science, Technology, and Innovative (MOSTI) Malaysia, for funding this research works. The first author acknowledges the National Science Fellowship (NSF) under Ministry of Science, Technology, and Innovative (MOSTI) Malaysia for the scholarship.

References

1. Estrela dos Santos J, Dockal ER, Cavalheiro TG. Thermal behavior of Shiff bases from chitosan. J Therm Anal Calorim. 2005;79(2):243–8.
2. Friedman M, Juneja VK. Review of antimicrobial and antioxidative activities of chitosan in food. J Food Protect. 2010;73(9):1737–61.
3. Jamil SM, Ali MW, Ripin A, Ahmad A. Metal removal from recovered base oil using chitosan bio-polymer. J Appl Sci. 2010;10(21):2725–8.
4. Martel-Estrada SM, Martinez-Perez CA, Chacon-Nava JG, Garcia-Casillas PE, Olivas-Armendariz I. Synthesis and thermo physical properties of chitosan/poly(di-lactide-co-glycosidic) composites, prepared by thermally induced phase separation. Carbohydr Polym. 2010;81(4):775–83.
5. Julkapli NM, Akil HM. Thermal properties of kenaf filled chitosan bio-composites. Polym Plast Technol Eng. 2010;49(2):147–53.
6. Ganji F, Abdekhodaie MJ. Synthesis and characterization of a new thermosensitive chitosan–PEG diblock copolymer. Carbohydr Polym. 2010;74:435–41.
7. Fan H, Wang L, Zhao K, Li N, Shi Z, Ge Z, Jin Z. Fabrication, mechanical properties and bio-compatibility of grapheme-reinforced chitosan composites. Biomacromolecules. 2010;11(9):2345–51.
8. RajivGandhi M, Viswanathan N, meenakshi S. Preparation and application of alumina/chitosan bio-composite. Int J Biol Macromol. 2010;47(2):146–54.
9. Venkatesan J, Kim S-K. Chitosan composite for bone tissue engineering-an overview. Mar Drugs. 2010;8(8):2252–66.
10. Danilchenko SN, Kalinkevich OV, Kuznetsov VN, Kalinkevich AN, Kalinichenko TG, Poddubny IN, Starikov VV, Sukhodub LF. Thermal transformations of the mineral component of chitosan biomaterials based on chitosan and apatite. Cryst Res Technol. 2010;45(7):685–91.
11. Peter M, Binulal NS, Nair SV, Selvamurugan N, Tamura H, Jayakumar R. Novel biodegradable chitosan-gelatin/nano-bioactive glass ceramic composite scaffolds for alveolar bone tissue engineering. Chem Eng J. 2010;158(2):353–61.
12. Habraken WJEM, Wolke JGC, Jansen JA. Ceramic composites as matrices and scaffolds for drug delivery in tissue engineering. Adv Drug Deliv Rev. 2007;59(4):234–48.
13. Julkapli NM, Akil HM. Influence of plasticizer on mechanical properties of kenaf filled chitosan bio-composites. Polym Plast Technol Eng. 2010;49(9):944–51.
14. Julkapli NM, Ahmad Z, Akil HM. Properties of kenaf filled chitosan bio-composites. Compos Interface. 2010;15(7):851–66.
15. Sashina ES, Janowska G, Zaborski M, Vnuchkin AV. Compatibility of fibroin/chitosan and fibroin clellose blends studied by thermal analysis. J Therm Anal Calorim. 2007;89(3):887–91.
16. Rao V, John J. Thermal behavior of chitosan/natural rubber latex blends TG and DSC analysis. J Therm Anal Calorim. 2008;92(3):801–8.
17. Gong Y, Yang G. Single polymer composites by partially melting recycled polyamide 6 fibers: preparation and characterization. J Appl Polym Sci. 2010;118(6):3357–83.
18. Salome Machoda AA, Martins VCA, Plepis AMG. Thermal and rheological behavior of collagen chitosan blends. J Therm Anal Calorim. 2002;67(2):491–8.
19. Hatakeyama H. Thermal analysis of environmentally compatible polymers containing plant components in the main chain. J Therm Anal Calorim. 2004;70(3):755–95.
20. Jaiswal MK, Banerjee R, Pradhan P, Bahadur D. Thermal behavior of magnetically modalized poly(*N*-isopropylacrylamide)-chitosan based nanohydrogel. Colloids Surf B. 2010;81(1):185–94.
21. Lee Y, Lee W. Degradation of trichloroethylene by Fe(II) chelated with cross linked chitosan in modified Fenton reaction. J Hazard Mater. 2010;176(1):187–93.
22. Chen M-C, Liu C-T, Tsai H-W, Lai W-Y, Chang Y, Sung H-W. Mechanical properties drug eluting characteristic and in vivo performance of a genipin cross linked chitosan polymeric stent. Biomaterials. 2009;30(9):5560–71.
23. Julkapli, NM, Ahmad, Z, Akil, HM. Preparation and characterization of 1,2,4,5-benzentetra carboxylic-chitosan. E-Polymer. 2010. Art no 077.
24. Nikonorov VV, Ivanov RV, Kil'Deeva NR, Bulatnikova LN, Lozinskil VI. Synthesis and characterization of cryogel of chitosan cross linked by glutaric aldehyde. Polym Sci A. 2010;52(8):828–34.
25. Peng H, Xiong H, Li J, Xie M, Liu Y, Bai C, Chen L. Vanillin cross linked chitosan microspheres for controlled release of resveratol. Food Chem. 2010;121(1):23–8.
26. Julkapli NM, Ahmad Z, Akil HM. Mechanical properties of 1,2,4,5-benzentetra carboxylic chitosan filled chitossan bio-composites. J Appl Polym Sci. 2011;121(1):111–26.
27. Julkapli NM, Akil HM. Degradability properties of kenaf filled chitosan bio-composites. Mater Sci Eng C. 2008;28(7):1100–11.
28. Julkapli NM, Ahmad Z, Akil HM. X-ray diffraction studies of cross linked chitosan with different cross linking agents for waste water treatment application. AIP Conf Proc. 2009;1202:106–11.

29. Julkapli NM, Akil HMd. X-ray diffraction (XRD) studies on kenaf filled chitosan bio-composites. AIP Conf Proc. 2008;989: 111–4.
30. Lopez FA, Merce ALR, Algvacli FJ, Lopez-Delgado A. A kinetic study on the thermal behavior of chitosan. J Therm Anal Calorim. 2008;91(2):633–9.
31. Martucci JF, Vazquez A, Ruseckaite RA. Nanocomposites based gelatin and montmorillonite. Morphological and thermal studies. J Therm Anal Calorim. 2007;89(1):117–22.
32. Chang PR, Jian R, Yu J, Ma X. Fabrication and characterization of chitosan nano particle/plasticized starch composite. Food Chem. 2010;120(3):730–40.
33. Taboada E, Cabrera G, Jimenez R, Cardenas G. A kinetic study of the thermal degradation of chitosan–metal complexes. J App Polym Sci. 2009;114(4):2043–52.
34. Ma L, Li G, Li L, Liu P. Synthesis and characterization of diethoxy phosphoyl chitosan. Int J Biol Macromol. 2010;47(7):578–81.
35. Dong J-J, Li S-D, Quan W-Y, Yang L, Fuand S-L, She X-D. Effect of degree of substitution on thermal stability of quaterized chitosan. J Polym Mater. 2010;27(2):125–33.
36. Mendes LC, Rodrigues RC, Silva EP. Thermal structural and morphological assessment of PVP/HA composites. J Therm Anal Calorim. 2010;101(3):899–905.